CrossMark

ORIGINAL ARTICLE

Comparing diffusion-weighted imaging and positron emission tomography for pulmonary nodules measuring from 1 to 3 cm in size

Hiroaki Nomori · Yue Cong · Hiroshi Sugimura · Yoshiaki Kato

Abstract

Purposes   To examine whether diffusion-weighted magnetic resonance imaging (DWI) is as useful as fluorodeoxyglucose positron emission tomography (FDG-PET) for discriminating between malignant and benign pulmonary nodules measuring less than 3 cm in size, as well as for predicting tumor aggressiveness.

Methods   PET and DWI were carried out on 87 pulmonary nodules measuring from 1 to 3 cm in size (66 NSCLCs and 21 benign nodules). The signal intensity (SI) of DWI was measured by the contrast ratio (CR) between the lesions and spinal cord, i.e. SI-CR. The maximum standard uptake value (SUV) of PET was measured by CR between the lesions and contralateral lung, i.e. SUV-CR.

Results   DWI and PET showed sensitivities of 0.86 and 0.71, and specificities of 0.90 and 0.81, respectively. While there was no significant difference in the specificity between the two, DWI showed a significantly higher sensitivity than PET ($p = 0.013$). While the difference in the sensitivity was significant in lung adenocarcinoma ($p = 0.012$), there was no difference in the other histological types. Both the SI-CR and SUV-CR were significantly higher in the tumors with either histological invasiveness or lymphatic metastasis than in those without.

Conclusions   DWI is thus considered to be useful, not only to diagnose NSCLCs, especially in lung adenocarcinoma, but also for predicting tumor aggressiveness as well as FDG-PET.

H. Nomori (✉) · Y. Cong · H. Sugimura
Department of General Thoracic Surgery, Kameda Medical Center, 929 Higashi-cho, Kamogawa, Chiba 296-8602, Japan
e-mail: hnomori@qk9.so-net.ne.jp

Y. Kato
Diagnostic Radiology, Kameda Medical Center, Chiba, Japan

Introduction

While CT is still the gold-standard for differentiating between benign and malignant pulmonary nodules, it sometimes lacks sufficient objectivity to achieve satisfactory results. To cover these shortcomings, positron emission tomography (PET) using ^{18}F-fluorodeoxyglucose (FDG) has been used to distinguish between benign and malignant ones. However, PET has also been known to sometimes provide false-negative results for well-differentiated pulmonary adenocarcinoma [1–6] and false-positive results for inflammatory nodules [3, 7].

On the other hand, recent advances in magnetic resonance (MR) gradient technology have led to the introduction of diffusion-weighted MR imaging (DWI), which provides excellent tissue contrast based on differences in the diffusion of water molecules among tissues and this modality is entirely different from ordinary T1- and T2-weighted MR images. Owing to the fact that the diffusion of water molecules is disturbed by intracellular organelles and macromolecules, any architectural changes in the proportion of extracellular to intracellular water molecules alter the values of the apparent diffusion coefficient (ADC) [8, 9]. Because malignant tumors have an increased cellularity, larger nuclei with more abundant macromolecular proteins, larger nuclear to cytoplasmic ratio, and less extracellular space in comparison to normal tissue, the values of ADC on DWI tend to decrease in malignant tumors, which thus allows for the imaging of malignant tumors by DWI [10, 11]. Until recently, the usefulness of DWI has been

Springer

reported in the imaging of various kinds of malignant tumors, including lung cancer [12–21].

While several authors have compared the images between DWI and PET in a small number of lung tumors [22–24], there have so far been few reports comparing the sensitivity and specificity of DWI and FDG-PET for diagnosing pulmonary malignancy. Mori et al. [18] reported DWI to have a similar sensitivity and a higher specificity compared to FDG-PET for distinguishing between malignant and benign pulmonary nodules; however, they examined lesions including those larger than 3 cm in size, which could thus be diagnosed easily without using DWI or PET.

While the quantitative analysis on DWI for differentiating between malignant and benign lesions has been made by measuring the values of the apparent diffusion coefficient (ADC) [12, 13], a recent study reported that the signal intensity (SI) of the lesion-to-spinal cord ratio showed a significantly higher sensitivity and specificity than ADC for differentiating between malignant and benign pulmonary nodules [24].

In the present study, to examine the usefulness of DWI in discriminating between non-small cell lung cancer (NSCLC) and benign pulmonary nodules measuring from 1 to 3 cm in size, we compared the sensitivity and specificity between DWI and FDG-PET, using SI of the lesion-to-spinal cord ratio (LSR) on DWI. In addition to examining the usefulness of DWI for predicting tumor aggressiveness, we also compared the SI on DWI between tumors with histological invasiveness and lymph node metastasis and those without.

Materials and methods

Eligibility

The study protocol for examining FDG-PET and DWI in patients with NSCLC prior to surgery was approved by the Ethics Committee of Kameda Medical Center. Informed consent was obtained from all patients after receiving a thorough explanation from their surgeons.

Patients

Between December 2012 and March 2014, 105 patients with pulmonary nodules prospectively underwent FDG-PET and DWI within a 4-week interval. The exclusion criteria for the study are as follows: (1) tumors with a ground-glass opacity (GGO) appearance, i.e. size of consolidation/tumor ratio less than 0.5; (2) tumors measuring less than 1 cm in size; and (3) tumors that were larger than 3 cm in size, of which the number of patients was 6, 4, and 18, respectively. As a result, 77 patients with 87 nodules measuring between 1 and 3 cm in size were selected (Table 1).

Table 1 Characteristics of pulmonary nodules less than 3 cm

Non-small cell lung cancer (n = 66)	
Histological types	
Adenocarcinoma	56
Squamous cell carcinoma	7
Adenosquamous carcinoma	1
Large-cell carcinoma	1
Large-cell neuroendocrine carcinoma	1
Lymphatic, vascular, or pleural invasion	
−	41
+	25
pN-stage	
N0	54
N1–2	12
Benign nodules (n = 21)	
Active inflammation	2
Old inflammation	19
Total	87

The nodules with a ground-glass opacity (GGO) appearance were excluded because they contained air, which makes the ADC value near 0. Of the 87 nodules, 66 were NSCLCs which were diagnosed histologically from surgical specimens. Of the 66 NSCLCs, 25 had lymphatic, vascular or pleural invasion and 12 had lymph node metastases. The 21 benign nodules were diagnosed as follows: 18 of them were diagnosed as old inflammatory nodules by their unchanged appearances for more than 2 years upon a review of retrospective chest X-ray films or CT, while the remaining three were diagnosed as active or old inflammation based on the pathological findings obtained from surgical specimens. The mean sizes of NSCLCs and benign nodules were 2.1 ± 0.6 cm (range 1.0–3.0 cm) and 1.5 ± 0.4 cm (range 1.0–2.7 cm), respectively.

Diffusion-weighted imaging (DWI)

All MR images were obtained with a 1.5 T superconducting system (MAGNETOM Avanto; Siemens, Germany). Conventional MR images and DWI were acquired during the same session. The conventional MR images consisted of a coronal T1-weighted sequence (repetition time [TR] ms/echo time [TE] ms, 177/4.7), and coronal and axial single-shot spin-echo T2-weighted sequences (1000/102). The T1- and T2-weighted images were acquired at a section thickness of 5 mm with 0 mm gap, with a 320×156 and 256×194 matrix, respectively, and a 263×350 mm and 280×350 mm field of view (FOV), respectively.

DWI was performed in the transverse plane using a spin-echo, echo-planar imaging sequence with pacing to each breath using the following parameters: TR/TE, 3100/73

with each breath, diffusion gradient encoding in 3 orthogonal directions; $b = 800$ s/mm^2; FOV 310 × 350 mm; 118 × 118 matrix; section thickness, 5 mm with 0 mm gap. Fusion images were made by sources of T2-weighted imaging and DWI to confirm the lesions.

PET-CT scanning

PET scanning in all patients was conducted at the Kameda Medical Center using an integrated PET/CT device (Discovery ST; GE Medical Systems). The patients were instructed to fast for at least 5 h before the intravenous administration of FDG. The dose of FDG was 185–230 MBq, which was determined by each patient's body mass index.

The acquisition time in 3-dimensional mode was 2.5 or 3 min per table position. Transaxial PET/CT data were acquired at a section thickness of 3.75 mm. PET image data were reconstructed iteratively using the ordered subsets expectation–maximization algorithm with segmented attenuation correction and CT data.

Measurement of signal intensity on DWI

The SI on DWI was measured using the region of interest (ROI) on the lesion using the AZE software program (Virtual Space, AZE Co., Tokyo Japan). The ROI was placed on the nodules. The maximum SI within the ROI was measured on each nodule. To eliminate any fluctuations of SI caused by the imaging conditions in each nodule, the contrast ratio of SI between lesions and the spinal cord (SI-CR) was calculated by the maximum SI of the lesion/mean SI of spinal cord at the same level of the lesion. To examine the variability of the spinal cord SI, the average value of SI at 6 levels of the spinal cord (each three levels above and below the lesion) was compared with the SI of the spinal cord at the same level of the lesion.

PET data analysis

PET data were evaluated semiquantitatively on the basis of the contrast ratio of SUV (SUV-CR), as described previously [25, 26]. Briefly, the ROI was placed on the nodules and at the equivalent point in the contralateral lung. The maximum SUV in the tumor ROI (T) and in the contralateral normal lung ROI (L) was measured. The SUV-CR of each nodule was calculated by T/L as an index of the FDG uptake.

Determining the cutoff value of SI-CR and SUV-CR

A receiver operating characteristic (ROC) curve was constructed using the StateMate software program (StateMate III: ATOMS Ltd., Tokyo Japan) to determine the cutoff values of SI-CR and SUV-CR to discriminate between NSCLC and benign nodules. Nodules with more than the cutoff values of SI-CR and SUV-CR were defined as positive on DWI and FDG-PET, respectively.

Statistical analysis

True-positive, true-negative, false-positive, and false-negative results for detecting pulmonary malignancies were compared between DWI and PET-CT. Sensitivity was
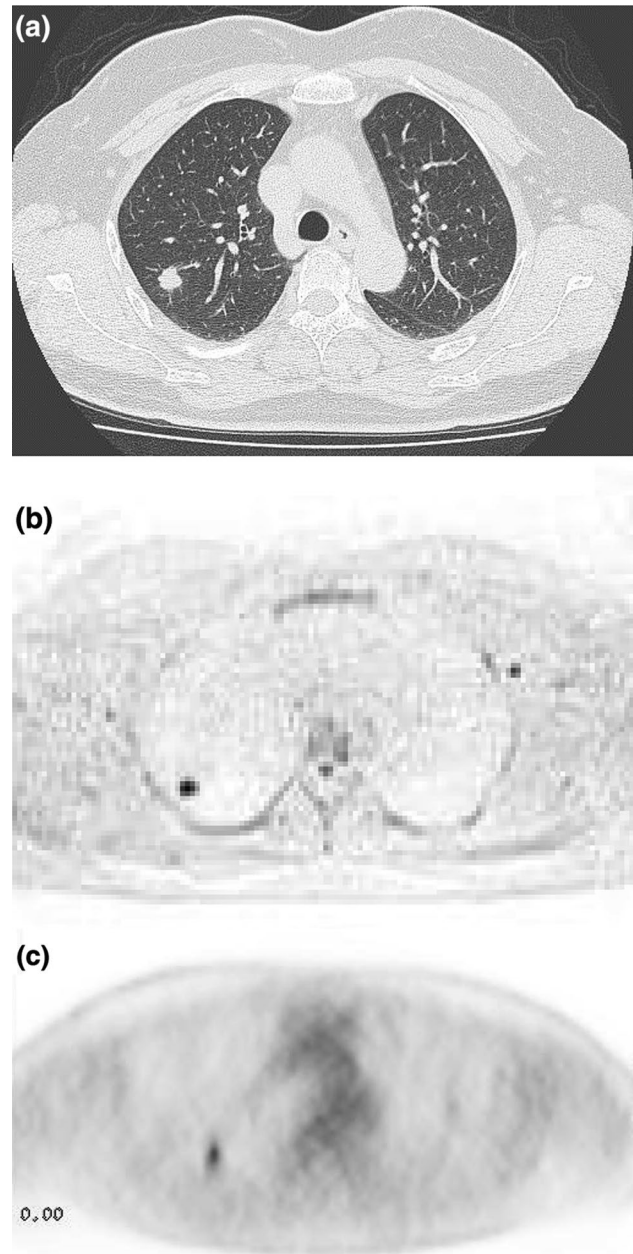

Fig. 1 Pulmonary adenocarcinoma: **a** CT image, **b** diffusion-weighted image, and **c** fluorodeoxyglucose positron emission tomography

calculated as true-positive/true-positive + false-negative, and specificity as true-negative/true-negative + false-positive. The differences in the sensitivity and specificity between DWI and PET were analyzed using McNemar's test. The differences in the SI of the spinal cord between the same level of the nodule and the other 6 levels were examined by the paired t test. The differences in the tumor size, SI-CR, and SUV-CR between tumors with histological tumor invasiveness or lymph node metastasis and those without were analyzed by the unpaired t test. A statistical analysis was performed using the StatMate software program (StateMate III: ATOMS Ltd., Tokyo Japan). All values in the text and tables are given as the mean ± standard deviation.

Results

DWI could image NSCLCs as well as FDG-PET (Fig. 1). The ROC curve for the diagnosis of malignant nodules showed the optimal cutoff value of SI-CR to be 0.45 and SUV-CR on PET to be 2.65. The mean values of SI of the spinal cord at the same level of nodules and the other 6 levels in each case were 64.0 ± 13.6 (range 39–90) and 65.1 ± 14.4 (range 37–88), respectively, and the difference was not significant.

Table 2 shows the results of DWI and PET in each histological type of the 66 NSCLCs, i.e. DWI was positive in 57 (86 %) and negative in 9 (14 %), while PET was positive in 47 (71 %) and negative in 19 (29 %). Of the 56 adenocarcinomas, a false-negative finding was shown in 9 (14 %) with DWI, while it was 19 (34 %) with PET. Of the 10 other histological types, none of the lesions (0 %) showed any false-negative findings with both DWI and PET.

Table 3 shows the results of DWI and PET in the 21 inflammatory nodules, i.e. DWI was positive in 3 nodules (14 %) and negative in 18 (86 %), while PET was positive in 4 (19 %) and negative in 17 (81 %).

Tables 4, 5, and 6 show the results of comparing between DWI and PET by McNemar's test. Table 4 shows the results of the diagnosis in NSCLCs. The DWI showed a significantly higher sensitivity than PET (0.86 vs. 0.71, $p = 0.013$). Table 5 shows the result of the diagnosis in lung adenocarcinoma and other histological types. The DWI showed a significantly higher sensitivity than PET for adenocarcinoma (0.84 vs. 0.66, $p = 0.012$), whereas all 10 of the other histological types showed a positive finding for both devices. Table 6 shows the result of the diagnosis in benign nodules. The specificities of DWI and PET were 0.90 and 0.81, respectively, of which the difference was

Table 2 Findings of diffusion-weighted imaging and positron emission tomography in malignant nodules

	DWI		PET		Total
	Positive	Negative	Positive	Negative	
Primary lung cancer					
Adenocarcinoma	47	9	37	19	56
Squamous cell carcinoma	7	0	7	0	7
Adenosquamous carcinoma	1	0	1	0	1
Large-cell carcinoma	1	0	1	0	1
LCNEC	1	0	1	0	1
Total	57	9	47	19	66

DWI diffusion-weighted imaging, *PET* positron emission tomography, *LCNEC* large-cell neuroendocrine carcinoma

Table 3 Findings of diffusion-weighted imaging and positron emission tomography in benign nodules

	DWI		PET		Total
	Positive	Negative	Positive	Negative	
Active inflammation	1	1	2	0	2
Old inflammation	1	18	2	17	19
Total	2	19	4	17	21

DWI diffusion-weighted imaging, *PET* positron emission tomography

Table 4 Correlation between diffusion-weighted imaging and positron emission tomography for diagnosing non-small-cell lung cancer

DWI	PET		Total
	True-positive	False-positive	
True-positive	45	12	57
False-positive	2	7	9
Total	47	19	66

DWI diffusion-weighted imaging, *PET* positron emission tomography

Table 5 Correlation between diffusion-weighted imaging and positron emission tomography for diagnosing lung adenocarcinoma and other histological types

DWI	PET		Total
	True-positive	False-negative	
Adenocarcinoma ($n = 56$)			
True-positive	35	12	47
False-negative	2	7	9
Total	37	19	56
Other histological types ($n = 10$)			
True-positive	10	0	10
False-negative	0	0	0
Total	10	0	10

DWI diffusion-weighted imaging, *PET* positron emission tomography

not significant ($p = 0.63$). The one nodule which showed a false-positive finding with DWI and a true-negative finding with PET showed granulomatous change in the surgical materials, i.e. suggestive of old tuberculosis.

Figure 2 shows the distributions of SI-CR and SUV-CR between 25 tumors with lymphatic, vascular, or pleural involvement and 41 without. The mean SI-CR of the invasive ones was 1.66 ± 0.84, which was significantly higher than 0.88 ± 0.6 of the non-invasive ones (Fig. 2a, $p < 0.001$). The mean SUV-CR of the former was 10.6 ± 7.7, which was significantly higher than 3.7 ± 2.7 of the latter (Fig. 2b, $p < 0.001$). The mean tumor sizes of the former and latter were 2.1 ± 0.5 and 2.0 ± 0.6 cm, respectively, and the difference was not significant.

Figure 3 shows the distributions of SI-CR and SUV-CR between 12 tumors with lymph node metastasis and 54 without. The mean SI-CR value of the metastatic ones was 1.76 ± 0.97, which was significantly higher than 1.04 ± 0.6 of the non-metastatic ones (Fig. 3a, $p < 0.001$). The mean SUV-CR of the metastatic ones was 13.5 ± 84, which was significantly higher than 4.7 ± 4.5 of the non-metastatic

Table 6 Correlation between diffusion-weighted imaging and positron emission tomography for diagnosing benign pulmonary nodules

DWI	PET		Total
	True-positive	False-positive	
True-positive	16	3	19
False-positive	1	1	2
Total	17	4	21

DWI diffusion-weighted imaging, *PET* positron emission tomography

ones (Fig. 3b, $p < 0.001$). The mean tumor sizes of the former and latter were 2.1 ± 0.5 and 2.0 ± 0.6 cm, respectively, and the difference was not significant.

Discussion

The present study highlights the following two points: (1) the SI-CR on DWI showed a higher sensitivity than SUV-CR on FDG-PET for NSCLCs measuring less than 3 cm in size, especially for adenocarcinoma, whereas there was no difference in the specificity between the two devices for benign nodules; and (2) the tumors with histological invasiveness or lymph node metastasis showed a significantly higher SI-CR on DWI than those without, similar to the findings for SUV-CR on PET.

The higher sensitivity of DWI compared with FDG-PET was dependent on that for lung adenocarcinoma, which could have been caused by the following: (1) some adenocarcinomas had a lower glucose metabolism, thus resulting in false-negatives by FDG-PET [1–6]; and (2) because the adenocarcinomas in the present study excluded adenocarcinoma in situ, all of their imaging on CT was solid type, but not GGO, which could be visualized by DWI because of low ADC values and a high SI, independent of their glucose metabolism. We therefore considered that while lung adenocarcinomas with poor invasiveness and a low proliferative activity could not be visualized by FDG-PET, because of their low glucose metabolism, DWI could visualize them except for adenocarcinoma with a GGO appearance.

The present study showed that the SI-CR on DWI showed significant relationships with tumor aggressiveness,

Fig. 2 The distributions of SI-CR on diffusion-weighted imaging (**a**) and SUV-CR on fluorodeoxyglucose positron emission tomography (**b**) between 25 tumors with lymphatic, vascular, or pleural involvement and 41 tumors without
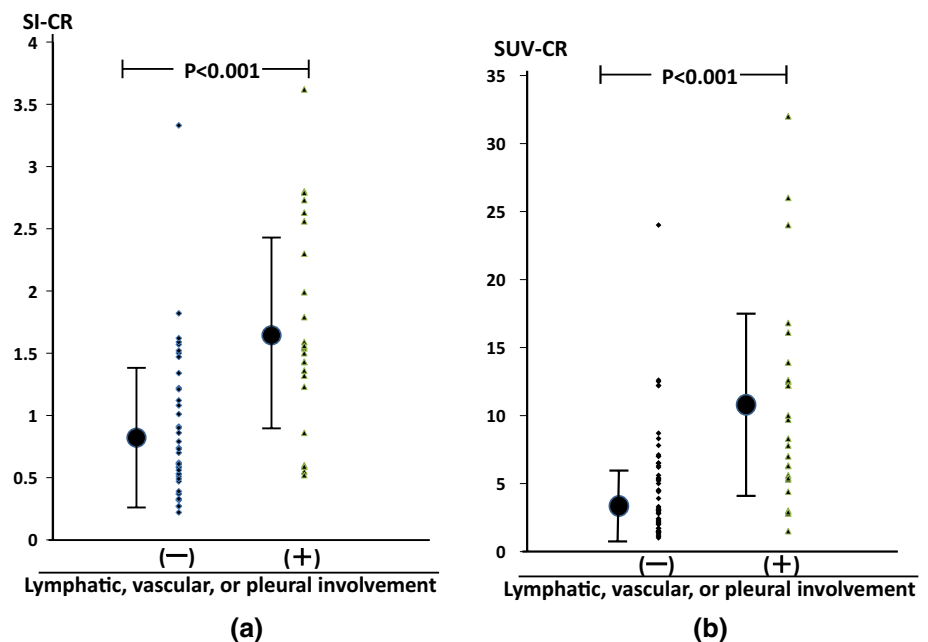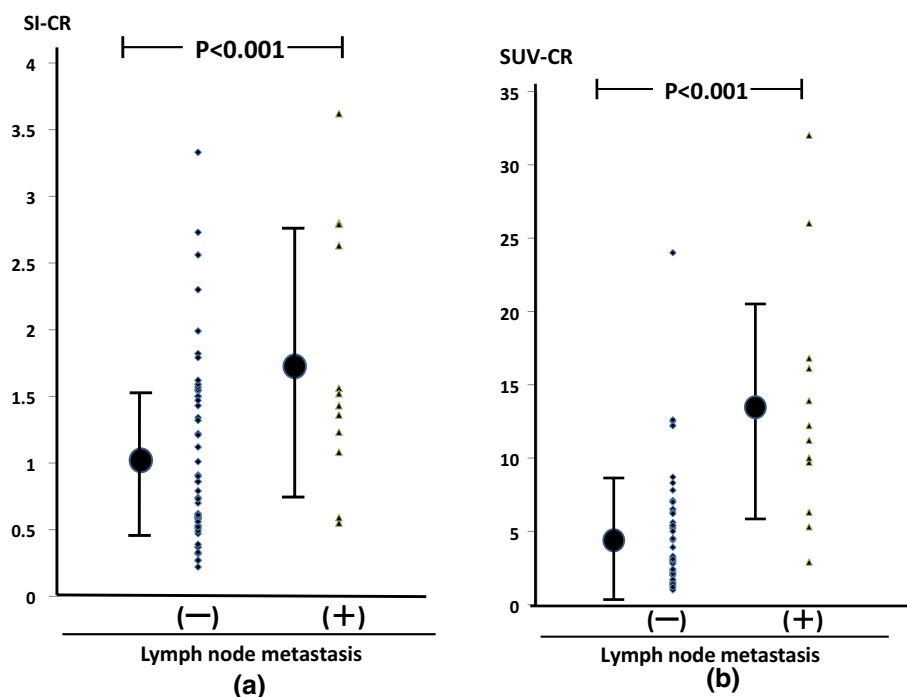
Fig. 3 The distributions of SI-CR on diffusion-weighted imaging (**a**) and SUV-CR on fluorodeoxyglucose-positron emission tomography (**b**) between 12 tumors with lymph node metastasis and 54 tumors without

as well as SUV-CR on FDG-PET. While Ohba et al. [19] reported that DWI could not predict the tumor invasiveness of NSCLC as well as FDG-PET, their study measured the minimum value of ADC on DWI in each tumor. In this study, we measured the SI-CR instead of ADC because of the following: (1) while the ADC measures the true value of diffusion of water molecules on DWI, it is sometimes affected by the position of ROI within tumors, because the ADC value with ROI including air within tumors or surrounding lung tissue will become lower than its true value; (2) while it cannot be denied that SI can be affected in T2 images, because of imaging on one b value ($b = 800$ in the present study), the maximum SI in ROI over the tumor is not affected by its positioning. As Wang et al. [27] described that ADC values cannot be measured for the lesions located adjacent to air-containing organs because of susceptibility artifacts, it is therefore difficult to measure the ADC value in tissue containing air. We consider that SI would be more reliable than ADC for analyzing DWI in NSCLC. However, it should be notified that the SI values in the present study are not common, because of a delicate difference in the SI among the devices of MRI.

While there was no significant difference in the specificities between DWI and PET, one benign nodule that was suggestive of old tuberculosis showed a false-positive finding with DWI and a true-negative finding with PET, which thus supported the results of our previous report showing false-positive findings for lymph node with granulomatous change [19]. It should be noted that nodules with

granulomatous change or dense fibrotic scar may show false-positive findings for DWI.

While the present study showed the superiority of DWI to PET for discriminating between malignant and benign nodules, DWI still has the following advantages over PET: (1) patients do not have to fast before examination; (2) there is no radiation exposure; (3) less time is required for the examination (30 min in DWI vs. 90 min in PET-CT); and (4) the cost is considerably less ($300 for DWI vs. $1400 for PET-CT in Japan). While FDG-PET is still superior to DWI for whole body imaging, this study showed that DWI could be used for discriminating between benign pulmonary nodules and NSCLC, especially adenocarcinoma, and even for predicting tumor aggressiveness as well as FDG-PET.

References

1. Higashi K, Nishikawa T, Seki H, Oguchi M, Nambu Y, Ueda Y, Yuasa K, Tonami H, Okimura T, Yamamoto I. Fluorine-18-FDG PET imaging is negative in bronchioloalveolar lung cancer. J Nucl Med. 1998;39:1016–20.
2. Cheran SK, Nielsen ND, Patz EF Jr. False-negative findings for primary lung tumors on FDG positron emission tomography: staging and prognostic implications. AJR. 2004;182:1129–32.
3. Nomori H, Watanabe K, Ohtsuka T, Naruke T, Suemasu K, Uno K. Evaluation of F-18 fluorodeoxyglucose (FDG) PET scanning

for pulmonary nodules less than 3 cm in diameter, with special reference to CT images. Lung Cancer. 2004;45:19–27.

4. Nomori H, Watanabe K, Ohtsuka T, Naruke T, Suemasu K, Kobayashi T, Uno K. Fluorine 18-tagged fluorodeoxyglucose positron emission tomographic scanning to predict lymph node metastasis, invasiveness, or both, in clinical T1 N0 M0 lung adenocarcinoma. J Thorac Cardiovasc Surg. 2004;128:396–401.

5. Watanabe K, Nomori H, Ohtsuka T, Naruke T, Ebihara A, Orikasa H, Yamazaki K, Uno K, Kobayashi T, Goya T. [F-18] Fluorodeoxyglucose positron emission tomography can predict pathological tumor stage and proliferative activity determined by Ki-67 in clinical stage IA lung adenocarcinomas. Jpn J Clin Oncol. 2006;36:403–9.

6. Imai K, Minamiya Y, Saito H, Motoyama S, Sato Y, Ito A, Yoshino K, Kudo S, Takashima S, Kawaharada Y, Kurihara N, Orino K, Ogawa J. Diagnostic imaging in the preoperative management of lung cancer. Surg Today. 2014;44:1197–206.

7. Goo JM, Im JG, Do KH, Yeo JS, Seo JB, Kim HY, Chung JK. Pulmonary tuberculoma evaluated by means of FDG PET: findings in 10 cases. Radiology. 2000;216:117–21.

8. Wang J, Takashima S, Takayama F, Kawashima S, Saito A, Matsushita T, Momose M, Ishiyama T. Head and neck lesions: characterization with diffusion-weighted echo-planar MR imaging. Radiology. 2001;220:621–30.

9. Sumi M, Takagi Y, Uetani M, Morikawa M, Hayashi K, Kabasawa H, Aikawa K, Nakamura T. Diffusion-weighted echoplanar MR imaging of salivary glands. AJR. 2002;178:959–65.

10. Takahara T, Imai Y, Yamashita T, Yasuda S, Nasu S, Van Cauteren M. Diffusion weighted whole body imaging with background body signal suppression (DWIBS): technical improvement using free breathing, STIR and high resolution 3D display. Rad Med. 2004;22:275–82.

11. Nasu K, Kuroki Y, Kuroki S, Murakami K, Nawano S, Moriyama N. Diffusion-weighted single shot echo planar imaging of colorectal cancer using a sensitivity-encoding technique. Jpn J Clin Oncol. 2004;34:620–6.

12. Murakami R, Sugahara T, Nakamura H, Hirai T, Kitajima M, Hayashida Y, Baba Y, Oya N, Kuratsu J, Yamashita Y. Malignant supratentorial astrocytoma treated with postoperative radiation therapy: prognostic value of pretreatment quantitative diffusion-weighted MR imaging. Radiology. 2007;243:493–9.

13. Woodhams R, Matsunaga K, Kan S, Hata H, Ozaki M, Iwabuchi K, Kuranami M, Watanabe M, Hayakawa K. ADC mapping of benign and malignant breast tumors. Magn Reson Med Sci. 2005;4:35–42.

14. Hayashida Y, Yakushiji T, Awai K, Katahira K, Nakayama Y, Shimomura O, Kitajima M, Hirai T, Yamashita Y, Mizuta H. Monitoring therapeutic responses of primary bone tumors by diffusion-weighted image: initial results. Eur Radiol. 2006;16:2637–43.

15. Reinsberg SA, Payne GS, Riches SF, Ashley S, Brewster JM, Morgan VA, deSouza NM. Combined use of Diffusion-Weighted MRI and 1H MR Spectroscopy to Increase Accuracy in Prostate Cancer Detection. AJR. 2007;188:91–8.

16. Dzik-Jurasz A, Domenig C, George M, Wolber J, Padhani A, Brown G, Doran S. Diffusion MRI for prediction of response of rectal cancer to chemoradiation. Lancet. 2002;360:307–8.

17. Matoba M, Tonami H, Kondou T, Yokota H, Higashi K, Toga H, Sakuma T. Lung carcinoma: diffusion weighted MR imaging—preliminary evaluation with apparent diffusion coefficient. Radiology. 2007;243:570–7.

18. Mori T, Nomori H, Ikeda K, Kawanaka K, Shiraishi S, Katahira K, Yamashita Y. Diffusion-weighted magnetic resonance imaging for diagnosing malignant pulmonary nodules/masses: comparison with positron emission tomography. J Thorac Oncol. 2008;3:358–64.

19. Ohba Y, Nomori H, Mori T, Ikeda K, Shibata H, Kobayashi H, Shiraishi S, Katahira K. Is diffusion-weighted magnetic resonance imaging superior to fluorodeoxyglucose-positron emission tomography in non-small cell lung cancer? J Thorac Cardiovasc Surg. 2009;138:439–45.

20. Nomori H, Mori T, Ikeda K, Kawanaka K, Shiraishi S, Katahira K, Yamashita Y. Diffusion-weighted magnetic resonance imaging can be used in place of positron emission tomography for N staging of non-small cell lung cancer with fewer false-positive results. J Thorac Cardiovasc Surg. 2008;135:816–22.

21. Ohno Y, Koyama H, Onishi Y, Takenaka D, Nogami M, Yoshikawa T, Matsumoto S, Kotani Y, Sugimura K. Non-small cell lung cancer: whole-body MR examination for M-stage assessment—utility for whole-body diffusion-weighted imaging compared with integrated FDG PET/CT. Radiology. 2008;248:643–54.

22. Komori T, Narabayashi I, Matsumura K, Matsuki M, Akagai H, Ogura Y, Aga F, Adachi I. 2-[Fluorine-18]-fluoro-2-deoxy-D-glucose positron emission tomography/computed tomography versus whole-body diffusion-weighted MRI for detection of malignant lesions: initial experience. Ann Nucl Med. 2007;21:209–15.

23. Lichy MP, Aschoff P, Plathow C, Stemmer A, Horger W, Mueller W, Steidle G, Horger M, Schafer J, Eschmann SM, Kiefer B, Claussen CD, Pfannenberg C, Schlemmer HP. Tumor detection by diffusion-weighted MRI and ADC-mapping—initial clinical experiences in comparison to PET-CT. Invest Radiol. 2007;42:605–13.

24. Uto T, Takehara Y, Nakamura Y, Naito T, Hashimoto D, Inui N, Suda T, Nakamura H, Chida K. Higher sensitivity and specificity for diffusion-weighted imaging of malignant lung lesions without apparent diffusion coefficient quantification. Radiology. 2009;252:247–54.

25. Nomori H, Watanabe K, Ohtsuka T, Naruke T, Suemasu K, Uno K. Visual and semiquantitative analyses for F-18 fluorodeoxyglucose PET scanning in pulmonary nodules 1 cm to 3 cm in size. Ann Thorac Surg. 2005;79:984–8.

26. Ohba Y, Nomori H, Shibata H, Kobayashi H, Mori T, Shiraishi S, Nakashima R. Evaluation of visual and semiquantitative assessments of fluorodeoxyglucose-uptake on PET Scans for the diagnosis of pulmonary malignancies 1 to 3 cm in Size. Ann Thorac Surg. 2009;87:886–91.

27. Wang J, Takashima S, Takayama F, Kawakami S, Saito A, Matsushita T, Momose M, Ishiyama T. Head and neck lesions: characterization with diffusion weighted echo-planar MR imaging. Radiology. 2001;220:621–30.